

# UC Office of the President

## Coastal Environmental Quality Initiative

### Title

Development of a dynamic optimal habitat model to describe the spatial and temporal habitat distributions of giant kelp, *Macrocystis pyrifera*

### Permalink

<https://escholarship.org/uc/item/7fn6708p>

### Authors

Senyk, Natalie Alexandra  
Sanchez, John

### Publication Date

2005-04-08

Peer reviewed

*CEQA Final Report*

Project Reference #: 02T CEQI 08 0098

**Development of a dynamic optimal habitat model to  
describe the spatial and temporal habitat distributions of  
giant kelp, *Macrocystis pyrifera***

## ABSTRACT

Development of a dynamic optimal habitat model to describe the spatial and temporal habitat distributions of giant kelp, *Macrocystis pyrifera*

By  
Natalie Alexandra Senyk

Forests of giant kelp, *Macrocystis pyrifera*, are common features of shallow rocky bottom habitats along California's coast. They function as an important marine habitat, supporting an abundance and diversity of life, and are commercially harvested. Long-term observations of giant kelp's (kelp) distribution and productivity have shown great temporal variability along with a declining trend over the last several decades in southern California. Hence, determining the distribution and persistence of kelp habitat requires an understanding of the factors driving variability in space and time. The role of time was examined by developing a model that utilizes remotely sensed data, along with other variables, to describe kelp's optimal habitat. The model is based on habitat preferences of kelp ("optimal habitat descriptors" or OHDs) and consists of a set of rules generated from observable environmental parameters, including substrate, bathymetry, monthly mean sea surface temperature, and monthly mean significant wave height. The study area included the northern Southern California Bight and offshore Channel Islands.

Four model variants were developed to describe optimal habitat by relaxing various assumptions. The nonsynergistic model ( $h_n$ ), the simplest model, assumed that each OHD functions independently spatially and temporally in the selection of optimal habitat. The synergistic model ( $h_s$ ) incorporated an inverse linear synergistic effect between wave height and the selection of optimal substrate. The model selected a wider range of substrate during months of reduced wave height and only rockier substrate as wave height increased. The final two models were developed by incorporating a temporal autocorrelation function into the  $h_n$  and  $h_s$  models, generating the nonsynergistic autocorrelative model ( $h_{na}$ ) and synergistic autocorrelative model ( $h_{sa}$ ) model, respectively. In these two variants, a location could persist through a single month of suboptimal conditions. The four models i.e.,  $h_n$ ,  $h_s$ ,  $h_{na}$  and  $h_{sa}$  each generated a 55-month time series of optimal habitat, spanning March 1998-September 2002, and were used to examine temporal variability and persistence.

All four models exhibited seasonal to interannual variability in optimal habitat. The annual cycle consisted of a summer season during which optimal habitat area reached a maximum with relatively minor monthly variability. The winter season was marked by significant declines in optimal habitat, corresponding with

increased wave heights generated by storms. Hence, winter storms play an important role in annual variability.

Interannual variability at various scales was also apparent. The models showed a marked decrease in optimal habitat during summer 1998, corresponding with the 1997-1998 El Nino event. Elevated sea surface temperatures were responsible for the decline in optimal habitat. An interannual trend was also apparent across all four models. It was marked by a less dynamic annual cycle during 2000-2002 relative to 1998-1999. Monthly mean optimal habitat area during the winter season was relatively greater during the latter period than the earlier period.

Model performance, characterized as the proportion of realized habitat identified from aerial surveys captured by models, was correlated with rocky substrate. The models captured the greatest proportion of realized habitat in rocky beds. The models also exhibited greater performance in the Channel Islands beds as compared to mainland beds.

Persistence was examined for those beds whose performance exceeded 75% for each of the four models. Persistence was more strongly correlated with rocky substrate in the synergistic models than the nonsynergistic models. All four models showed greatest persistence with a SST range between 12-14°C.

## TABLE OF CONTENTS

List of Tables

List of Figures

1. Introduction
2. Data and Methods
  - 2.1 Optimal Habitat Descriptor (OHD) Data Sets
  - 2.2 Model Description
  - 2.3 Optimization of OHD parameters, **T**
  - 2.4 Characterizing Model Performance
3. Results
  - 3.1 Optimized **T**
  - 3.2 Study Area--Optimal habitat (ho) timeseries
  - 3.3. Subregions-- Optimal habitat (ho) timeseries
    - 3.3.1 Oregonian Subregion
    - 3.3.2 Californian Subregion
    - 3.3.3 Islands Subregion
  - 3.4 Model Performance
  - 3.5 Persistence
4. Discussion
5. Conclusions
6. References

## 1. Introduction

Giant kelp (*Macrocystis pyrifera*) is a common and important shallow subtidal macroalgae, forming underwater forests, or beds, along rocky reefs between central California and Baja California, Mexico. It is a keystone species, functioning as a food source, nursery ground and protection for a wide variety of species (Carr 1989; Leet et al. 2001). It is also harvested for the abalone aquaculture, and as well as for extraction of alginates, which are used in products such as cosmetics, paint, salad dressing, ice cream, and paper.

Giant kelp (kelp) is a brown macroalgae, with a heteromorphic lifecycle consisting of a haploid gametophyte stage and a diploid sporophyte stage, the large plants forming familiar beds. An individual plant consists of a rootlike holdfast that attaches to hard substrates. A long stalk, or stipe, acts as an attachment for the leaf-like fronds, which are the major site of photosynthetic activity. Gas-filled bladders called pneumatocysts support the kelp plant and allow it to grow toward the sea surface. A plant may grow to lengths of 60 m with its upper fronds forming a dense canopy at the surface.

Kelp's preferred habitat is well defined by several environmental variables. It is typically located on rocky substrate, consisting of <20% sand (Graham et al. 1997). However, it has also been shown to occur with moderate amount of sand on reefs of 1m relief (Deysher et al. 2002).

However, substrate is known to vary with the amount of wave exposure. Typically, where wave height is reduced, kelp can be found over more diverse substrate (review in Brown et al. 2002; Brown et al. 1999)

In regions of reduced wave exposure, such as the protected shoreline of Santa Barbara County, California, kelp can also occur over softer substrate, attaching to worm tubes or remains of old holdfasts (Leet et al. 2002). Giant kelp prefers depths less than 40 m (Dayton et al. 1999). Its deeper depth limit is controlled by light intensities, needing atleast 1% of the surface irradiance (Foster and Schiel 1985).

Kelp requires <17 °C (Foster and Shiel 1985; Deysher and Dean 1986; Tegner *et al* 1997). Density of sporophyte recruitment and growth rates tend to decline in these conditions. Water temperature functions as a proxy for nitrate and is the best indicator of harvestable kelp biomass (Tegner et al. 1996). It is inversely correlated with nitrate concentration in southern California (Jackson 1977; Zimmerman and Kremer 1984). Temperatures exceeding 16°C are correlated with nitrate depletion, which can lead to a decrease in sporophyte recruitment, reduced growth rates and mortality of individual kelp plants. The length of time of low-

nitrate, warm temperature conditions will affect the magnitude of effects. Growth can become nutrient limited during summer months. During these periods of low seawater nitrate concentrations, kelp can sustain internal nitrogen concentrations for about one month of and hence delaying growth declines (Brown et al. 1997).

The general location of kelp beds has been temporally consistent, but the extent, or actual distribution, of those beds has varied greatly over annual to interannual time scales (Ugoretz 2002), as reflected in harvest rates. ISP Alginates, Inc., the company that harvests kelp, conducts monthly aerial surveys of kelp biomass in California's beds. The kelp bed boundaries are defined by the California Department of Fish and Game's (CDFG) administrative beds (Beds) (Table 1; Figure 1). The kelp biomass time series spans 1967 to the present. During 1970-1979, the average state-wide harvest was nearly 157,000 tons, while the average harvest between 1980-1989 was 80,400 tons.

Many factors affect the productivity and distribution of kelp over a range of spatial and temporal scales. Biological, physical and anthropogenic factors have both direct and synergistic effects. Herbivore grazing can affect local scale variability by limiting the distribution of kelp. In some cases, grazing can lead to a complete removal of kelp beds, leaving an 'urchin barren'. Competition for benthic habitat with understory algae can prevent kelp recolonization once an area has been decimated by other factors (Dayton and Tegner 1984).

Physical factors can lead to regional-scale variability in kelp distribution over annual to interannual frequencies. Annual regional-scale events, such as storms can lead to kelp mortality and reduction in kelp productivity. In southern California, the Mediterranean climate is marked by storms during the winter (Ford 2000). These events are characterized by increased wave exposure and storm surge, which can break fronds and uproot entire kelp plants. The uprooted plants can entangle and further remove more kelp. In southern California, entanglement with storm-dislodged kelp is a major cause of mortality (Dayton et al. 1984).

Low nutrient oceanographic conditions also have an effect on kelp productivity and distribution. In southern California, summer months are usually marked by depressed upwelling, leading to warm-water, low-nitrate conditions in the euphotic zone. Such conditions stress kelp, causing a decrease in density of sporophyte recruitment and growth, and potentially mortality (Jackson 1977; Deysher and Dean 1986; Zimmerman and Kremer 1986).

Interannual variability in kelp distribution and productivity is correlated with ENSO events. The large-scale, low-frequency El Nino events affect the severity of storms and warm-water, low-nitrate conditions (Dayton and Tegner 1984; 1987;

Ladah et al. 1999). The increase in the number and intensity of storms can lead to decimation of kelp along its entire range. The severity is typically greater in southern California relative to central California. El Nino events are reflected in harvest rates. The low harvest rates between 1980-1989 was attributed to the 1982-1984 El Nino event and subsequent storms, as well a 200-year storm during January 1988 (Leet et al. 2001).

Several strong El Nino events have occurred in the last 20 years. The 1982-1984 event devastated kelp survival. A combination of reduced nitrate levels during summer and several severe storms decimated kelp in southern California (Dayton and Tegner 1984). Subsequently, sea urchin grazing increased, preventing re-seeding of kelp in areas where it had previously been, preventing recolonization. Some regions have never been recolonized. The 1997-1998 El Nino was the warmest in the last two decades (Leet et al. 2001).

An interdecadal trend of increasing frequency, duration and intensity of warm-water El Nino events and a corresponding decrease in cool-water La Nina events since the mid 1970s is evident (Tegner et al. 2001). This 'regime-shift', sometimes referred to as the Pacific Decadal Oscillation, is associated with increased sea surface temperature (Roemmich and McGowan 1995) and a shift in mean location of SST isotherms to the north (Tegner et al. 2001) in the northeastern Pacific. The southern limit of kelp's distribution in Baja California has also shifted further north since the 1982-1984 El Nino event (Ladah et al. 1999).

Anthropogenic factors can also affect kelp distribution and productivity. Discharges of wastewater and thermal byproducts and coastal development can increase turbidity and sedimentation. Increased sedimentation can prevent kelp spore attachment to the substrate, cause smothering, or scour microscopic sporophytes thereby reducing success (Devinny and Vorse 1978). As a result, kelp, growth, productivity, and survival may decline and mortality may increase (Dean and Deysler 1983).

The role of anthropogenic factors is difficult to assess given concurrent natural variability over annual to interannual scales and a lack of a time series of kelp distribution to characterize variability. Of concern is the increasing coastal population, which is predicted to grow XX in the next XX years, which may magnify the impact of anthropogenic factors on the coastal ecosystem. Along southern California's mainland, the kelp beds appear to have declined relative to historic levels potentially due to anthropogenic factors (Leet et al. 2001). The status of several regions of kelp beds are of concern, including the kelp beds along Santa Barbara/Ventura (Leet et al. 2001).



Concern about protecting and restoring important coastal species and habitats, such as kelp, have stimulated a shift in management from a single-species to ecosystem-based approach (NAS 2000; NOAA 2000). Marine protected areas (MPAs) are a zoning tool, restricting to various degrees human activities within their boundaries that are implemented with traditional single-species management. Marine reserves are the strictest type of MPA, allowing no extractive activities within it, such as fishing, oil drilling. By taking an ecosystem-based approach, MPAs protect the species, interactions, and ecological linkages that traditional single-species management cannot.

In southern California, a network of MPAs was implemented by the California Fish and Game Commission in 2003 stimulated by a public concern that the health and status of the coastal ecosystem was in decline relative to historic levels. The network was established in the Channel Islands National Marine Sanctuary (CINMS), a 6 nmi boundary along 5 southern California islands, including San Miguel, Santa Rosa, Santa Cruz, Anacapa, and Santa Barbara Islands. The region is a biologically diverse region, located in the transition of the cold water Oregonian biogeographic province to the north and the warmer water Californian biogeographic province. It has historically been a productive fishing area for a wide range of fish and invertebrates. The high productivity sustains a wide range of marine mammals and sea birds. The CINMS MPA network consists of 10 marine reserves and 2 conservation areas located around the islands. The conservation areas allow limited take.

The MPA network was established to meet a variety of goals, including protecting ecosystem biodiversity. The objective focused on protecting representative and unique marine habitats, ecological processes, and species of interest. A network consisting of 10 marine reserves and 2 conservation areas, which allow limited extractive activities, was established to represent the biogeographic provinces and placed around the five islands.

An integral component in developing the CINMS MPA network were habitat maps of the region's species of interest. Habitat representations are typically the central focus of site selection schemes of MPAs, because the lifecycle of the majority of economically important fish species can be reduced to several general habitat-related patterns (Koenig et al 2000). Large-scale habitat maps allow managers to visualize the spatial distribution of habitats, aiding in the planning of networks of MPAs and allowing habitat fragmentation to be monitored (Mumby and Harborne 1999).

In the CINMS MPA process, the potential distribution of kelp, identified as a species of interest, was mapped using maximum extent identified using aerial photographs of the region between 1980 and 1989 (Ecoscan 1989). The maximum

extent map provides presence/absence information but does not provide any information on persistence or temporal dynamics. The temporal variability of the coastal ecosystem, as indicated in the characterization of temporal scales of kelp, due to anthropogenic disturbance, oceanographic events and community changes can have a significant effect on species' distributions, and hence the value of habitat delineated in maps (Chelton et al 1982; Roemmich and McGowan 1995; Carroll et al 1999; Walters and Bonfil 1999). Hence, the development of MPAs requires information regarding spatial and temporal dynamics of habitats and the variability that exists in coastal marine systems (NAS 2000; Rieser 2000). A need exists to address the dynamic effects of ecosystem processes through time-series analyses (Mumford 1992; Allee et al. 2000). Characterization of temporal dynamics in habitat maps can aid in identifying persistent habitat. It may also assist in distinguishing and characterizing the relative impacts of natural variability versus anthropogenic-caused trends.

The primary objective of this project was to examine the role of time in kelp's optimal habitat distribution and characterize persistent habitat. The study area was the Channel Islands region, including mainland coast north of Point Conception to Ventura and the four northern Channel Islands (San Miguel, Santa Rosa, Santa Cruz and Anacapa Islands) (Figure 1).

The approach was to develop a model that utilizes existing data sets to gain an understanding of and quantify the spatial and temporal variability associated in the coastal region affecting kelp's optimal habitat. Optimal habitat is defined for these purposes as that area where ambient environmental conditions are suitable for an organism to exist during a given month, or simply where an organism can exist. It is delineated by optimal habitat descriptors (OHD), which are the environmental variables that characterize kelp's preferred habitat, such substrate type and wave exposure.

The approach of this research project was to develop an optimal habitat ( $h_o$ ) model that utilizes existing data sets to gain an understanding of and quantify spatial and temporal variability associated with the coastal region and affecting kelp habitat. The model utilizes data collected by other research programs and publicly available. The goals were to assemble data sets that could characterize the temporal and/or spatial scales of OHDs, develop a model to describe space/time distributions of optimal habitat based upon a set of rules and OHDs, validate the results with aerial surveys, and analyze spatial and temporal patterns and persistence of kelp's optimal habitat. Application of the OHDs in delineating optimal habitat requires an understanding of species-habitat relationships. OHDs can function as surrogates for identification of species' distributions if the relationship between habitat and a species' physiological tolerances can be

constrained. Descriptor thresholds, or parameters, can then be used to delineate locations of optimal habitat.



Figure 1. Study Area. The study area includes a region south of Morro Bay to Ventura, California and the northern Channel Islands, including (west to east): San Miguel, Santa Rosa, Santa Cruz, and Anacapa Islands. The California Department of Fish and Game (CDFG) Administrative Beds in the study area are delineated in green. See Table 1 for Bed names.

Table 1. List of CDFG Beds included in the study region.

<b>CDFG Administrative Bed #</b>	<b>Bed Name</b>
18	Ventura
19	Rincon Point
20	Carpinteria
21	Summerland
22	Santa Barbara
23	Santa Barbara Breakwater
24	Arroyo Burro
25	Hope Ranch
26	Goleta
27	Coal Oil Point
28	Naples
29	El Refugio
30	Tajiguas
31	Gaviota
32	San Augustine
33	Point Conception
34	Point Arguello
106	Santa Barbara Island
109	Anacapa Island
110	Santa Cruz Island (N)
111	Santa Cruz Island (W)
112	Santa Cruz Island (N)
113	Santa Rosa Island (SE)
114	Santa Rosa Island (SW)
115	Santa Rosa Island (NW)
116	Santa Rosa Island (NE)
117	San Miguel Island (S)
118	San Miguel Island (N)
202	Purisma Point
203	Point Sal

## 2. Data and Methods

### *Optimal Habitat Descriptor (OHD) Data sets*

Data sets used as OHDs in developing the optimal habitat model were selected by the following criteria: (1) previous studies have shown correlations between the distribution of kelp and the OHD, (2) data was publicly available, (3) the temporal scale and/or spatial extent of each OHD data set was appropriate for this project. The OHD data sets needed to encompass the study area. From a temporal perspective, OHD data sets that can vary on sub-monthly scales were considered dynamic and sub-monthly time series were required to characterize their temporal dynamics.

Four OHD data sets were selected using these criteria, including substrate type, bathymetry, wave height and sea surface temperature (SST). Substrate type and bathymetry were defined as static OHDs in that they were assumed to not change over monthly to interannual scales. Wave height and SST were defined as dynamic OHDs because they have sub-monthly temporal scales of variability. Substrate grab samples collected by Continental Shelf Data Systems and the United States Geological Survey (USGS) within the Santa Barbara Channel were used to characterize rocky substrate. An interpolated grid was created from these points, consisting of the probability of encountering rocky substrate (R). Bathymetry (B) was generated from USGS Digital Line Graphs and NOAA GEODAS bathymetry points. Advance Very High Resolution Radiometer (AVHRR) imagery, collected at the University of California Santa Barbara (UCSB), were used to generate monthly mean SST composites. Daily significant wave height predictions, generated by the Scripps Institute of Oceanography's Coastal Data Information Program, were used to generate monthly mean significant wave heights (H). Monthly SST and H composites spanned March 1998 and September 2002.

Further processing of the four OHD data sets was needed to make them spatially compatible. Each data set had a different spatial extent and resolution, so each was first clipped to a common spatial extent and then resampled to a 60 meter grid. The grid resolution was confined by B, which had the greatest resolution. The data sets were now referenced to a common coordinate system, where a row, column index  $i,j$  referenced the same point in each OHD data set.

### *$h_0$ Model Description*

Four variants of an  $h_0$  model were developed (Table 2). All models utilized the OHD data sets to delineate monthly optimal habitat composites. The literature survey of kelp's preferred habitat was used to establish a threshold, or parameter,  $T$   $\{T = T_R, T_B, T_{SST}, T_H\}$  for each OHD. The four  $h_0$  models consisted of simple binary logic rules using the four OHDs and associated parameters to delineate

optimal habitat. Each model generated a 55-month time series of optimal habitat, spanning the length of the dynamic OHDs.

The four  $h_o$  models differed in the assumptions incorporated into the binary logic rules. All four models assume that OHDs decide the location of optimal habitat. The first model, the nonsynergistic model ( $h_n$ ), also assumed that no synergistic effects exist between OHDs and no temporal correlation exists in the selection of optimal habitat. The second model, the synergistic model ( $h_s$ ) incorporated a synergistic function between R and H in the selection of optimal habitat. The synergistic function assumed a linear relationship between H and  $T_R$ , the R parameter, such that as H increased  $T_R$  also increased and only rockier substrate was selected as optimal habitat.

The final two models build upon the  $h_n$  and  $h_s$  models, but incorporate a time lag in the selection of optimal habitat. An autocorrelation function, which is the correlation of a variable with itself over successive time intervals, in the final two models allowed for persistence of optimal habitat through a single month of suboptimal environmental conditions. These models are the nonsynergistic autocorrelative ( $h_{na}$ ) model and the synergistic autocorrelative ( $h_{sa}$ ) model. In these models,  $h_o$  could persist through a single month of suboptimal conditions. Hence,  $h_o = \{h_n, h_s, h_{na}, h_{sa}\}$ . All four models generate a 55 month time series, spanning the temporal window of SST and H.

### **Optimization of OHD parameters, T**

In order to support the selection of **T** from literature-defined ranges, an optimization procedure was developed. The objective was to select **T** such that the resulting  $h_o$  time series generated the greatest correspondence between model predictions of  $h_o$  distribution and the realized ( $h_r$ ), distribution of kelp. The ISP Alginates, Inc. biomass time series was used to optimize **T** because it spanned the model's temporal frequency and period, and included data on Beds in the study area. The optimization assumed that a linear relationship exists between  $h_o$  area and biomass within a Bed and the **T** generating the greatest significant  $r^2$  value was used to delineate  $h_o$  in the models.

CDFG aerial surveys of kelp canopy, or realized habitat ( $h_r$ ), were used to examine the strength and significance of the relationship between  $h_r$  distribution and biomass. Periodic aerial surveys of California's shallow subtidal region are part of the California Kelp Resources Survey and are used to monitor the States' kelp resources. The aerial photography collected during the surveys captures kelp's distribution, which is then processed into ESRI Arcview software products. Two CDFG surveys, conducted during 1989 and 1999, were plotted against biomass for Beds within the study area and showed a fit of  $r^2 = 0.34$   $p < 0.001$  for 1989 and  $r^2 =$

0.39  $p < 0.001$  for 1999 (Figure 2). The significance and strength of the relationship supported the optimization assumption.

The optimization consisted of randomly selecting  $T$  from a uniform distribution with bounds defined by the literature survey and generating an  $h_o$  time series. Each Bed's monthly  $h_o$  area was then plotted against corresponding biomass

A linear regression of each Bed's monthly  $h_o$  area versus corresponding biomass was calculated and the strength and significance of the relationship was evaluated. The  $T$  that generated the greatest significant  $r^2$  value was used to generate the final  $h_o$  time series. The optimization was run separately for the nonsynergistic models e.g.,  $h_n$  and  $h_{na}$  and synergistic models e.g.,  $h_s$  and  $h_{sa}$ , generating a nonsynergistic  $T$  and a synergistic  $T$ . The final model products consisted of four 55-month  $h_o$  timeseries;  $h_n$ ,  $h_s$ ,  $h_{na}$ ,  $h_{sa}$ .

#### *Characterizing $h_o$ Model Performance*

Model performance was characterized by comparing model predictions of  $h_o$  distribution to  $h_r$  distribution. The 1999 CDFG aerial survey was used to characterize  $h_r$ . Performance was measured by proportion of  $h_r$  captured by each  $h_o$  model within each Bed in the study area. The percent overlap between  $h_r$  and  $h_o$  in each Bed was then plotted against each Bed's mean  $R$ , mean  $H$  and mean SST to characterize model performance in relation to the OHDs. Mean  $H$  and mean SST were calculated using the three monthly composites corresponding with the period when the aerial survey was conducted (October-December 1999).



**Table 2. A summary of the four optimal habitat ( $h_0$ ) models**

<b><math>h_0</math> Model</b>	<b><math>h_0</math> Variable</b>	<b><math>h_0</math> Model Description</b>
Nonsynergistic	$h_n$	Nonsynergistic; No autocorrelation
Synergistic	$h_s$	Synergistic effect between R and H; No autocorrelation
Nonsynergistic Autocorrelative	$h_{na}$	Nonsynergistic, autocorrelative
Synergistic Autocorrelative	$h_{sa}$	Synergistic effect between R and H; Autocorrelative

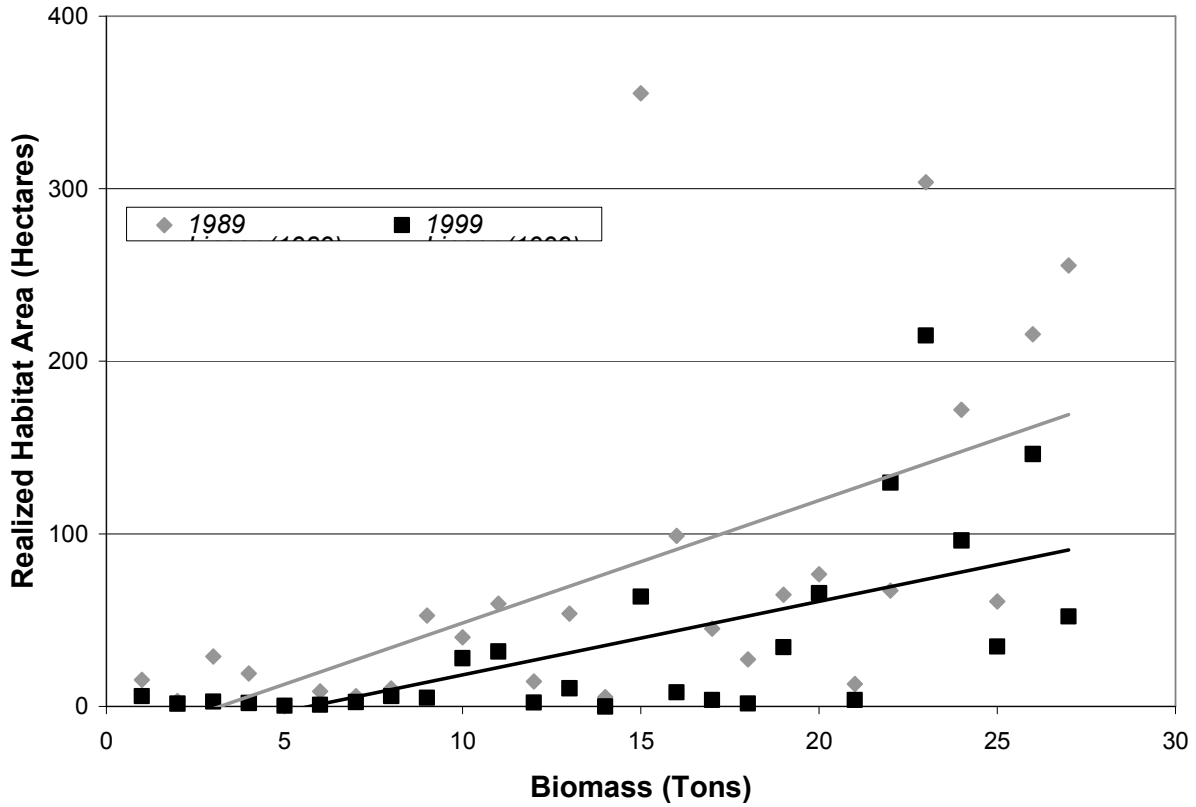


Figure 2. Linear regression of realized habitat area ( $h_r$ ) vs. biomass.  $h_r$  was characterized using 1989 and 1999 CDFG aerial surveys of California's shallow subtidal region. Biomass was characterized using ISP Alginates, Inc. data.

### 3. Results

#### *Study Area--Optimal habitat ( $h_o$ ) time series*

The four models'  $h_o$  time series were examined. Figure 3 shows monthly  $h_o$  area for the entire study area. Several observations can be made regarding the models. First, the autocorrelative models e.g.  $h_{na}$  and  $h_{sa}$  are a 'smoothed' version of their related non-autocorrelative models e.g.  $h_n$  and  $h_s$ . The autocorrelative models are less dynamic, exhibiting less variability between months but show similar annual to interannual patterns as their related models. Because the autocorrelative models are similar to their related models, the following discussions will primarily focus on comparisons between the  $h_n$  and  $h_s$  models.

The magnitude of  $h_o$  area varied between the  $h_n$  and  $h_s$  models. The  $h_s$  model selected significantly greater area relative to the  $h_n$  model. The  $h_s$  model had a mean 9,231 hectares/month while the  $h_n$  model had a mean 4,258 hectares/month. April 1999 was the only month when all models converged on the amount of  $h_o$  area.

All four models did exhibit an annual cycle with two distinct seasons. The season of minimum area occurred in late winter/spring (winter season), corresponding with the occurrence of winter storms.  $h_o$  area then increased to a maximum in summer/late fall season (summer season). This season of increased area exhibited less variability relative to the winter/early spring season. The  $h_n$  model was more dynamic than the  $h_s$  model between seasons. The  $h_n$  model exhibited more than a 60% difference in  $h_o$  area between seasons while the  $h_s$  model exhibited a 20% difference.

An interannual trend was also evident in all four models. The trend was marked by decreased seasonal and annual variability during the latter period of the time series e.g., 2000-2002 relative to the earlier period e.g. 1998-1999. The summer season was less variable between months during the latter period. Also, mean monthly  $h_o$  area during the winter season was relatively greater during the latter period. The  $h_n$  model exhibited a 31% difference between the two periods' average winter season  $h_o$  area while the  $h_s$  model exhibited a 16% difference.

#### *Subregions— $h_o$ time series*

The study area was broken up into three subregions and  $h_o$  time series were similarly examined. The subregions were delineated based on well-defined boundaries in physical oceanographic patterns and marine populations as well as distance from human influence (Leet et al. 2002; Ugoretz 2002). The Oregonian subregion was spatially defined as the area north of Point Conception, California and included Beds 33, 34, 202 and 203. The Californian subregion was defined as

the California mainland coast south of Point Conception, including Beds 18-34. Finally, the Islands subregion was defined as all of the Beds around San Miguel Island, Santa Rosa Island, Santa Cruz Island, and Anacapa Islands, including Beds 109-118.

Several model differences evident at the scale of the study area also appeared in the subregions. First, similar to the entire study area, the autocorrelative models were a 'smoothed' version of their related non-autocorrelative models so discussions will continue to focus on the  $h_n$  and  $h_s$  models (Figure 4). Second, the  $h_s$  model consistently captured more area than the  $h_n$  model across all three subregions. Third, several significant declines were evident across subregions and models during which models converged on the magnitude of  $h_o$  area. All models showed a decline during summer 1998, corresponding with an El Nino and in April 1999, corresponding with a winter storm.

The relative magnitude of annual variability between the  $h_n$  and  $h_s$  models was not uniform across subregions. In the Californian subregion, the  $h_s$  model exhibited greater relative annual variability. This differed from the Oregonian and Islands subregions, as well as the study area, where the  $h_n$  model exhibited greater relative annual variability.

#### *Oregonian Subregion*

The Oregonian subregion exhibited relatively large seasonal variability, leading to a prominent annual cycle across all models (Figure 4a). The  $h_n$  model frequently declined to zero, predicting no  $h_o$  area during those months. These declines typically occurred during the winter/early spring season. These windows of suboptimal conditions occasionally occurred for up to two consecutive months, marked by declines in the  $h_{na}$  model.

#### *Californian Subregion*

As stated previously, the Californian subregion was the only subregion where the  $h_s$  model exhibited relatively greater annual variability, leading to a prominent annual cycle (Figure 4b). The  $h_n$  model was almost static, periodically declining during both seasons. The El Nino decline in late summer 1998 was most evident in this subregion. During this time, both the  $h_n$  and  $h_s$  models declined to zero.

#### *Islands Subregion*

Similar to the Oregonian subregion, the  $h_n$  model exhibited relatively greater annual variability for the Islands subregion (Figure 4c). The amplitude of the annual cycle is greatly reduced in the  $h_s$  model.

### *Effect of Synergistic Function*

The synergistic function had a more profound effect on temporal dynamics and model performance than the autocorrelation function. The synergistic function used monthly mean significant wave height to generate the  $T_R$  parameter, or the threshold that defined the lower limit of rocky substrate in the selection of  $h_o$ . As  $H$  increased,  $T_R$  also linearly increased so that the range of  $R$  values decreased. The effect of the synergistic function was usually a dampened annual cycle. The synergistic models often exhibited reduced temporal variability relative to the nonsynergistic models. This was evident in the study area, as well as in the Oregonian and Islands subregions. The synergistic function acted as a type of buffer in these areas, allowing locations of rockier substrate to persist through months of increased wave heights when the nonsynergistic models exhibited decreases in  $h_o$  area. These periods of increased wave heights tended to occur during the winter season, when storms generated increased  $H$ . Hence, the synergistic models were relatively more resilient to winter storms in these areas.

The synergistic models' relatively dampened annual cycle was not seen in all areas. In the Californian subregion, the synergistic models were more dynamic, exhibiting relatively greater annual variability as compared with the nonsynergistic models. The nonsynergistic models were almost static, with few declines in  $h_o$  area during both summer and winter seasons. The greatest discrepancy in area between the synergistic and nonsynergistic models also occurred in the Californian subregion. A 3 to 4 order magnitude difference was evident across most of the time series (Table 3; Figure 4).

The combined effect of softer substrate and low wave heights in the Californian subregion offers insight on the effect of the synergistic function. The subregion has relatively softer substrate ( $R < 0.2$ ) and lower mean monthly significant wave heights relative to the Oregonian and Islands subregions (Figures 5 and 6). The relatively greater proportion of softer substrate does not affect the nonsynergistic models because it does not exceed the nonsynergistic  $T_R$  parameter ( $T_R = 0.27$ ). However, the effect of lower wave heights causes the nonsynergistic models to capture more persistent area because wave height does not typically exceed 0.7 m, the nonsynergistic  $T_H$  parameter. Hence, wave height plays a more minor role in driving temporal variability in the Californian subregion. Indeed, optimal habitat is relatively stable, showing a few declines in both the summer and winter season.

The effect of the Californian subregion environmental conditions is markedly different in the synergistic models. The subregion's low wave heights, which cause the nonsynergistic models to have a more stable habitat distribution, along with softer substrates cause the synergistic models' greater relative variability. The average significant wave heights in the subregion range from 0.11-0.61 (mean =

0.36, std dev = 0.25). The corresponding TR parameter range is 0.11-0.29, which includes a significant proportion of the Californian subregion.

It is the softer substrate, that the nonsynergistic models do not capture, along with lower wave heights that causes the synergistic model's greater temporal variability in the Californian subregion. The combined effect of soft substrate and low wave heights on the synergistic function is a lower  $T_R$  parameter, and a wider range of optimal substrate. Hence, the synergistic models capture a greater amount of area than the nonsynergistic models.

However, the softer substrate is more sensitive to small increases in wave height than rockier substrate. A relatively small increase in wave height causes a increase in the TR parameter such that the softer substrate may be excluded. Wave heights range

It is the relatively greater area of softer substrate in the Californian subregion, that the nonsynergistic models miss, that causes the synergistic models to capture more area than the nonsynergistic models. The combined, synergistic effect of softer substrate and low wave height causes the synergistic models to exhibit greater temporal variability.

### *Model Performance*

All models overpredicted the amount of area relative to  $h_r$ , characterized by the CDFG 1999 aerial survey, for both the entire study area and the three subregions. Table 3 shows  $h_r$  area calculated using the 1999 aerial survey and  $h_o$  area predicted by the four models. The synergistic models predicted more area relative to the nonsynergistic models across all regions. For the study area and the Islands subregion, the synergistic models predicted twice as much area relative to the nonsynergistic models. The greatest discrepancy between models occurred in the Californian subregion where predictions ranged by a factor of four. The greatest discrepancy between  $h_o$  and  $h_r$  occurred in the Oregonian subregion, where the nonsynergistic models captured an order or magnitude more area and the synergistic models captured two orders of magnitude greater area.

A portion of the discrepancy between  $h_r$  and  $h_o$  area can be explained by the mismatch in scale of the aerial photography and the  $h_o$  time series.  $h_r$  has a resolution of 2 meters, which is determined by the aerial photography. The  $h_o$  models are mapped onto a 60 meter resolution grid.

Model performance, characterized by the proportion of  $h_r$  captured by  $h_o$ , varied by subregion. The synergistic models captured a greater proportion of  $h_r$  relative to

the nonsynergistic models across all subregions (Table 4). The nonsynergistic models captured the same proportion across all regions. All models performed poorly in the Californian subregion and only slightly better in the Oregonian subregion. All models captured the greatest proportion of  $h_r$  in the Islands subregion.

The relationship between model performance and OHDs was examined. All models showed a correlation with R and H. However, R exhibited greater relative correlation with model performance. No relationship existed between model performance and SST because the period examined corresponded with relatively cooler waters of late fall that did not exceed  $T_{SST}$  parameter. Hence SST does not limit the selection of optimal habitat during this time period. Also, no relationship existed between B and model performance.

Beds with greater mean R exhibited greater model performance (Figure 7a; Table 5). Beds with lower mean R correlated with a large range in model performance. The nonsynergistic models' performances had the greatest correlation ( $r^2 = 0.66$ ;  $p < 0.001$ ) with R. The  $h_s$  and  $h_{sa}$  models showed lower relative correlation ( $r^2 = 0.59$  and  $r^2 = 0.52$ , respectively), but were still significant ( $p < 0.001$ ).

Similarly, the nonsynergistic models showed relatively greatest correlation with H ( $r^2 = 0.30$ ;  $p < 0.001$ ) (Figure 7b; Table 5). The  $h_s$  and  $h_{sa}$  models showed lower correlation ( $r^2 = 0.23$  and  $r^2 = 0.21$ , respectively), although those relationships were also significant ( $p < 0.001$ ).

Table 3. Area comparisons between the 1999 CDFG kelp canopy aerial survey ( $h_r$ ) and the four ho models. A maximum ho composite was generated for each model using the three month period of October-December 1999, corresponding with the CDFG aerial survey. Area units are hectares. The table compares the area estimates for the entire study region as well as for each of the three biogeographic regions.

		<b>SUBREGIONS</b>		
<i>(All areas in hectares)</i>	<b>Entire Study Region</b>	<b>Oregonian</b>	<b>Californian</b>	<b>Islands</b>
$h_r$	908	12	135	761
$h_n$	4746	731	279	3735
$h_{na}$	4833	793	279	3760
$h_s$	8171	1117	876	6178
$h_{sa}$	8722	1183	1147	6392

Key:

$h_r$ —1999 kelp canopy aerial survey

$h_n$ —nonsynergistic model

$h_s$ —synergistic model

$h_{na}$ —nonsynergistic autocorrelative model

$h_{sa}$ —synergistic autocorrelative model

Table 4. Proportion of the 1999 CDFG kelp canopy aerial survey e.g.  $h_r$  identified by each model. The  $h_r$  total column shows the area measured by the aerial survey for both the study region and the biogeographic regions. The  $h_n$ ,  $h_{na}$ ,  $h_s$ , and  $h_{sa}$  columns show the proportion of  $h_r$  that each model captures for both the study region and the biogeographic regions.

	$h_r$ <b>Total</b>	$h_n$	$h_{na}$	$h_s$	$h_{sa}$
<b>Study Area</b>	908	0.47	0.47	0.63	0.69
<b>SUBREGIONS</b>					
<b>Oregonian</b>	12	0.17	0.17	0.46	0.54
<b>Californian</b>	135	0.04	0.04	0.18	0.35
<b>Islands</b>	761	0.55	0.55	0.72	0.77



Table 5. Linear regression parameters of model performance and R and H.  
R is the probability of rocky substrate and H is wave height

<b>OHD</b>	<b>h<sub>o</sub> Model</b>	<b>Linear Model</b>	<b>r<sup>2</sup> (p &lt; 0.001)</b>
R	h <sub>n</sub> /h <sub>na</sub>	y = 105x - 1	0.66
R	h <sub>s</sub>	y = 123x + 11	0.59
R	h <sub>sa</sub>	y = 121x + 15	0.52
H	h <sub>n</sub> /h <sub>na</sub>	y = 94x - 15	0.30
H	h <sub>s</sub>	y = 101x - 3	0.23
H	h <sub>sa</sub>	y = 101x + 1	0.21

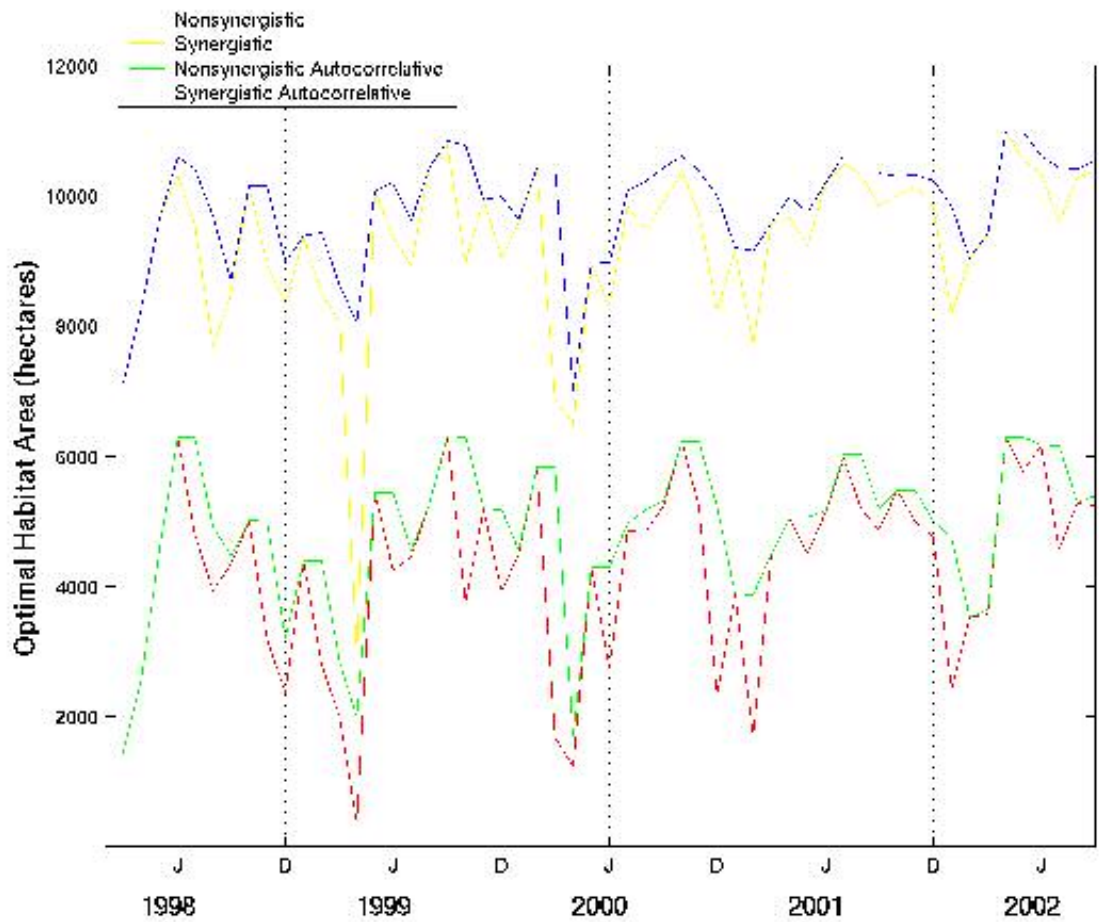


Figure 3. Timeseries of optimal habitat area per month for the entire study area. Timeseries spans March 1998 to September 2002 with June and December months delineated.

LEGEND

Yellow line --  $h_s$  model      blue line --  $h_{sa}$  model  
 red line --  $h_n$  model      green line --  $h_{na}$  model

q

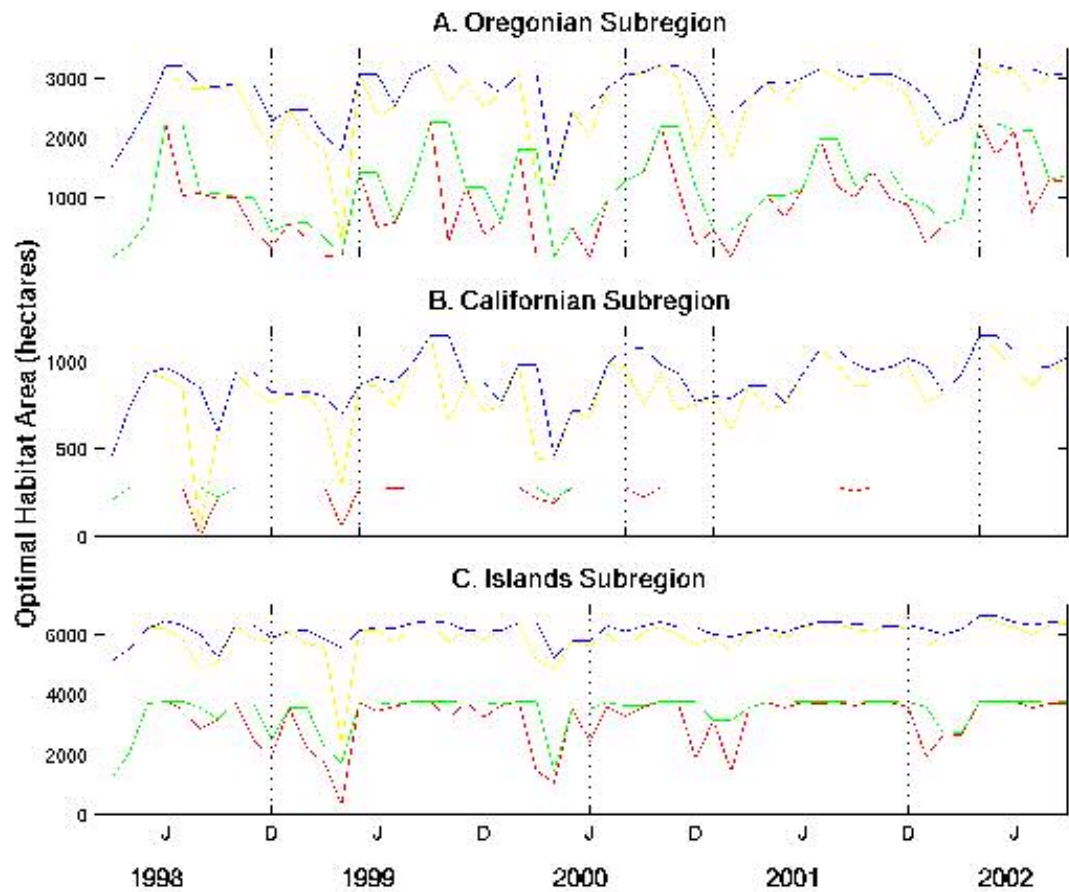


Figure 4. Timeseries of optimal habitat area per month for the Oregonian, Californian, and Islands subregions. Subregions were delineated by a distinct biogeographic boundary and proximity from human populations. The time series of monthly optimal habitat area (hectares) span March 1998 to September 2002 with June and December months delineated to show the two distinct seasons. A. Oregonian Subregion B. Californian Subregion C. Islands Subregion

LEGEND

Yellow line --  $h_s$  model

blue line --  $h_{sa}$  model

red line --  $h_n$  model

green line --  $h_{na}$  model

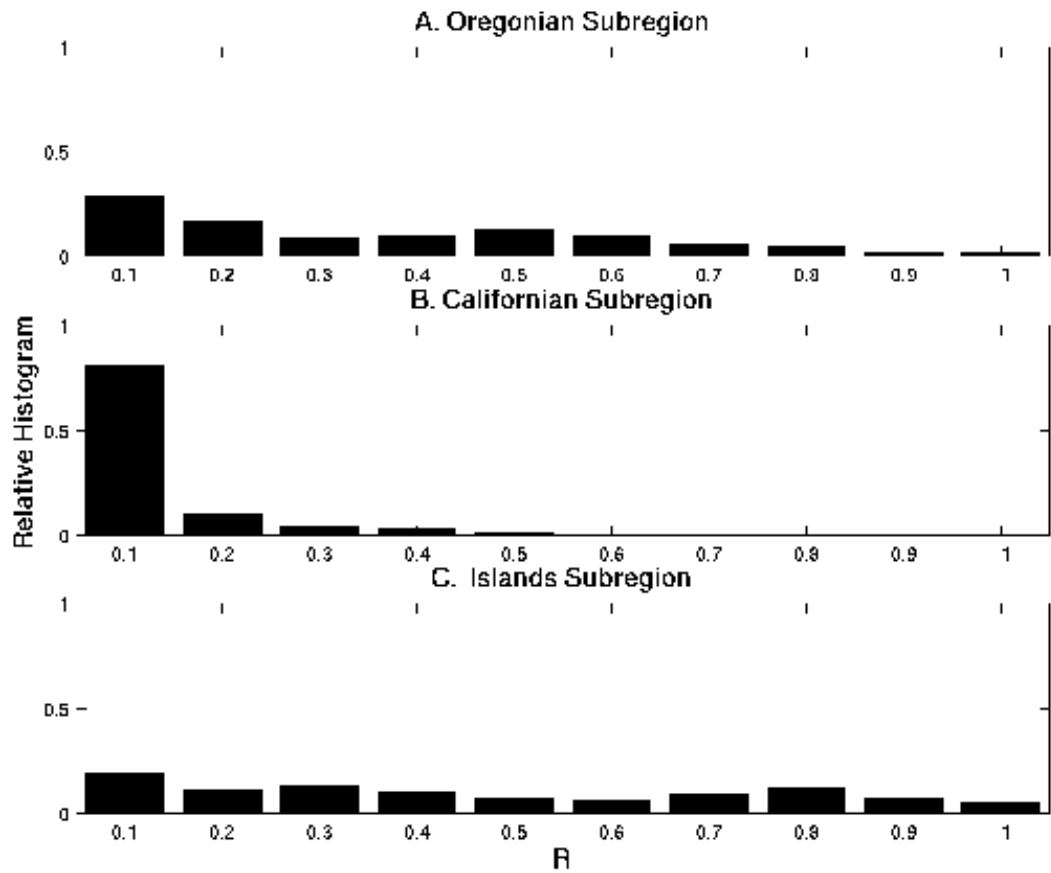


Figure 5. Relative histogram of rocky substrate (R) in the three subregions. R is the probability of encountering rocky substrate. Only the shallow subtidal portion (depth >15 meters) of each subregion was used in this characterization to reflect the depth range of optimal habitat. The Californian subregion has the greatest amount of soft substrate, with over 70% of the area has an  $R < 0.20$ .

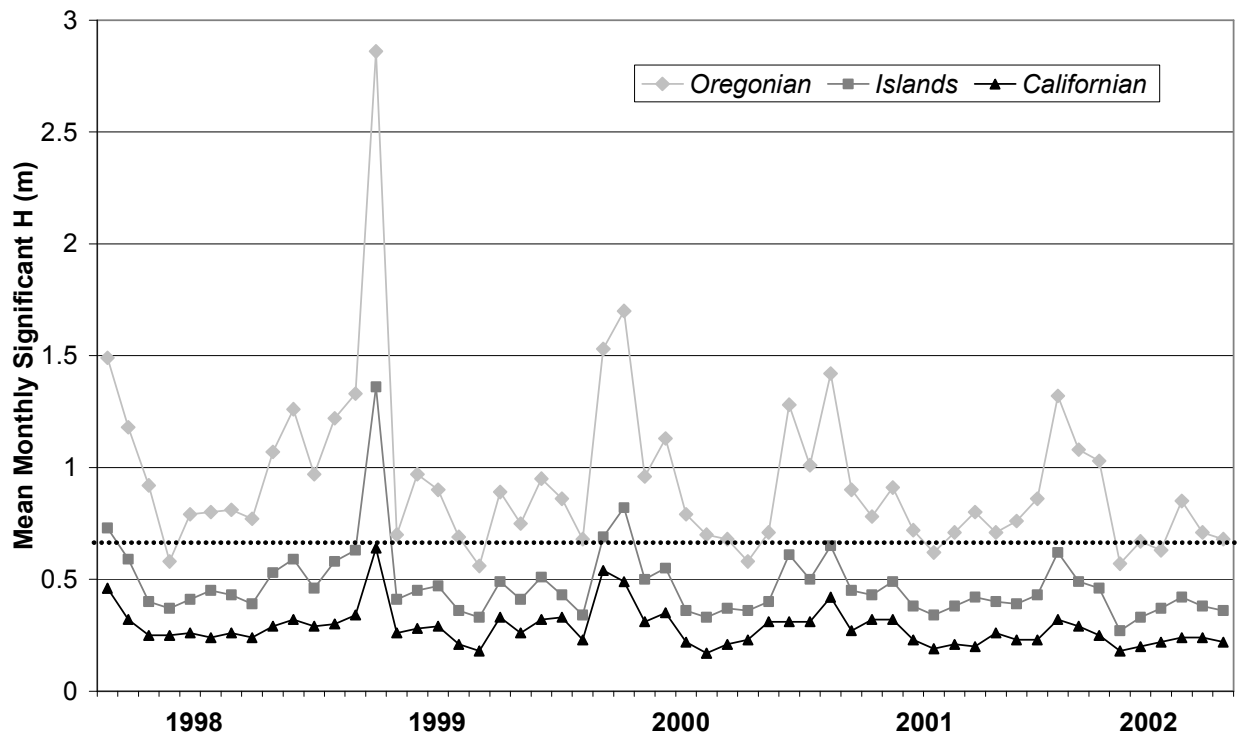


Figure 6. Time series of each subregion's mean monthly significant wave height (H). Only the shallow subtidal portion (depth >-15 meters) of each subregion was used in this characterization to reflect the depth range of optimal habitat. Light gray is the Oregonian subregion, dark gray is the Islands subregion and black is the Californian subregion. The horizontal dashed line represents the nonsynergistic  $T_H$  parameter (0.7m). The plot shows that the Californian subregion has the lowest wave heights, and the Oregonian has the greatest wave heights, where wave heights frequently greatly exceed the nonsynergistic  $T_H$ .

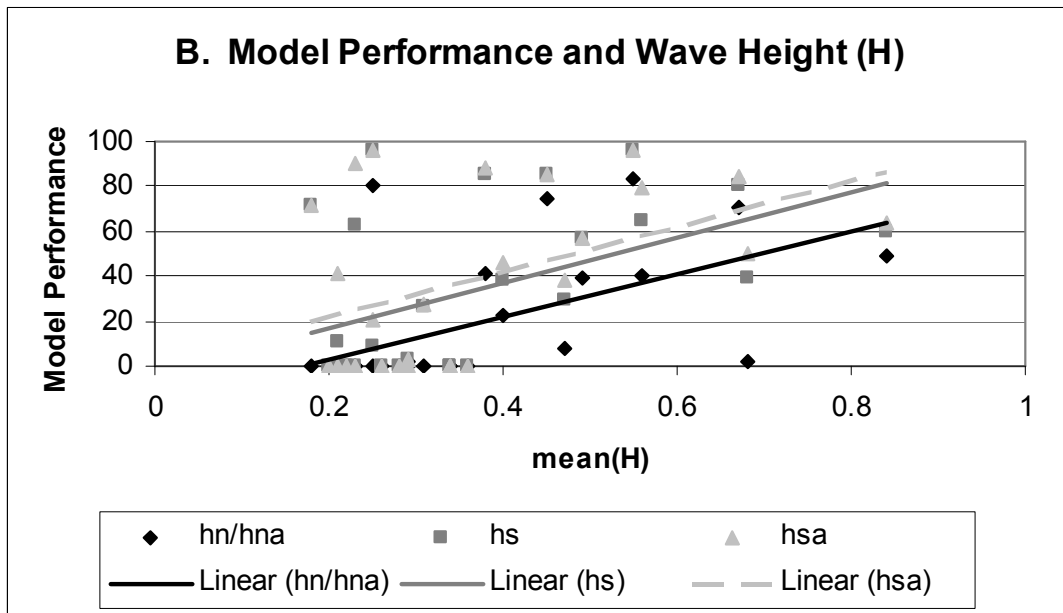
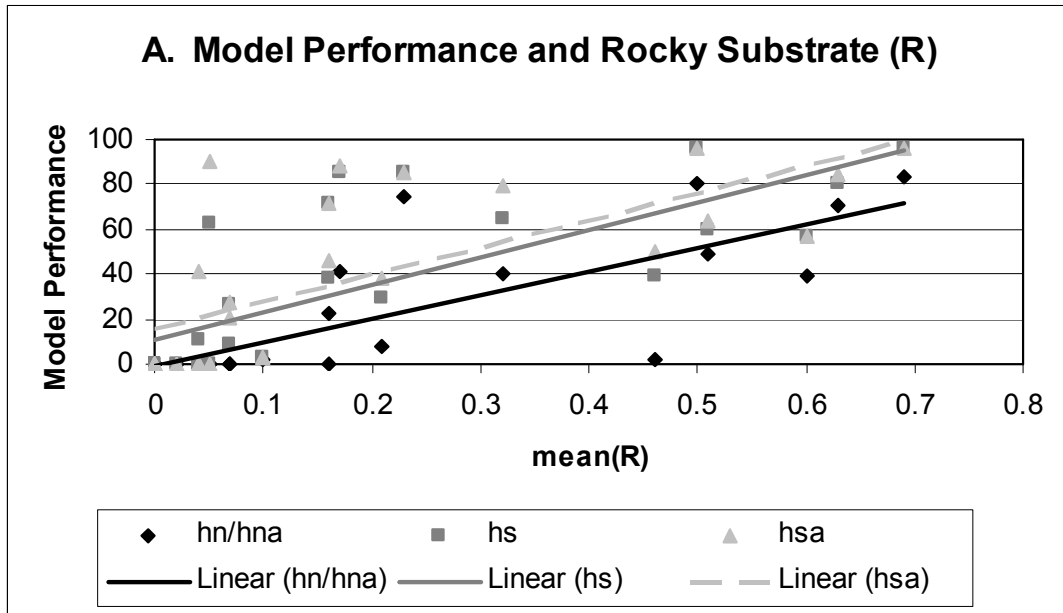


Figure 7. Relationship between model performance and optimal habitat descriptors (OHDs). Model performance, mean probability of rocky substrate (mean R), and mean monthly maximum wave height were calculated for each of the 29 CDFG administrative beds (Bed) in the study area. Model performance is the proportion of realized habitat ( $h_r$ ) captured by the four models in each Bed. The 1999 CDFG kelp aerial survey was used to calculate  $h_r$ . A. Mean probability of rocky substrate B. Mean monthly wave height (H).

## 4. Discussion

Four optimal habitat ( $h_o$ ) models were developed by relaxing two assumptions in the selection of optimal habitat ( $h_o$ ). The first relaxed assumption was that no synergistic effects exist between the optimal habitat descriptors, or OHDs, when selecting optimal habitat. Each OHD functions independently in the selection of  $h_o$ . The second relaxed assumption was that  $h_o$  was not temporally correlated, or autocorrelated, with itself. Hence, the selection of  $h_o$  was independent of the previous month. The simplest model, the nonsynergistic ( $h_n$ ) model, incorporated both assumptions. The synergistic ( $h_s$ ) model slightly relaxed the first assumption by incorporating a linear synergistic function between wave height (H) and the selection of rocky substrate. The nonsynergistic autocorrelative ( $h_{na}$ ) model evolved from the  $h_n$  model but incorporated an autocorrelation function such that the selection of  $h_o$  was correlated to the previous month's conditions. Finally, the synergistic autocorrelative ( $h_{sa}$ ) model, which evolved from the  $h_s$  model, relaxed both assumptions.

The two assumptions had different effects on  $h_o$  temporal dynamics and model performance. The autocorrelation function had a minor effect on temporal dynamics and model performance. The autocorrelative models e.g.,  $h_{na}$  and  $h_{sa}$  exhibited a similar temporal pattern as their related models e.g.,  $h_n$  and  $h_s$ , respectively. However, the autocorrelative models were not affected by high frequency (<2 months) variation. Hence, these models were more resilient and impacted only by longer periods of suboptimal conditions.

Although they differed in their assumptions, all four models showed an interannual trend in  $h_o$  area. The trend was apparent to varying degrees at both the study area and subregion scales. The interannual trend coincides with a negative event in all models corresponds with a La Nina event that is evident in the multivariate ENSO index (MEI) (Figure 8).

All models overpredicted the amount of  $h_o$  area relative to  $h_r$  area, as well as underpredict localized patches of kelp canopy in the 1999 CDFG kelp canopy aerial surveys. The degree to which models exhibit a mismatch varies by subregion. Possible sources of discrepancy and error may include: biological controls (such as predation and competition), differences in scale between realized habitat and optimal habitat, model assumptions, Binary 'presence/absence' model approach in selecting optimal habitat, the linear assumption of biomass and cover used in optimization, and/or substrate data.

Rocky substrate was responsible for most of the locations missed by the models because these locations are not included during any month of the time series

across all regions because the majority of missed locations did not exceed models'  $T_R$  parameters and were thus excluded.

The interpolated substrate grid of probability of rocky substrate in these locations did not exceed the respective models'  $R$  parameter. These underpredicted  $h_r$  locations are characterized as soft substrate. Because soft substrate can be dynamic, influenced by waves, it does not provide an attachment source for the kelp's holdfast to adhere. Kelp can grow on sandy substrate in locations sheltered from wave exposure (Leet et al. 2001). Old holdfasts can function as attachment sites.

The accuracy of the substrate grid may contribute to the discrepancy between  $h_r$  and  $h_o$ . The average minimum distance of 300 m between substrate samples in the shallow subtidal region limits the ability to characterize smaller scale variability of substrate. The result is that the substrate grid may incorrectly characterize areas because of lack of sampling. The substrate map also does not characterize substrate dynamics. Lack of characterization of substrate dynamics may also contribute to the models' inaccuracy. The substrate may shift, rocky areas may be covered by sand.

Suggestions for model improvement include:

- Improved substrate data—finer scale and a measure of temporal dynamics
- More frequent kelp canopy aerial surveys
- Development of a probabilistic model
- Consideration of other OHDs—irradiance, turbidity;
- Field studies to characterize and quantify OHD synergistic effects and their role in affecting kelp dynamics

### *Persistence Analysis*

Persistence patterns were analyzed for those Beds where each model captured 75% or more of  $h_r$ , which was defined by the 1999 CDFG kelp aerial survey. The threshold was selected because it roughly separated two modes in model performance. Persistence patterns were characterized by the average number of continuous months of  $h_o$  for those Beds exceeding the threshold for each model. The average number of consecutive months was then plotted against  $R$ , mean SST, and maximum  $H$  for each model. Mean SST and maximum  $H$  were global statistics of the entire time series and calculated for each location within Beds that exceeded the 75% persistence threshold. Both nonsynergistic models exceeded the 75% threshold for two Beds: 115 and 116. The  $h_s$  model exceeded the threshold for five



Beds: 110, 111, 114, 115, 116. The  $h_{sa}$  model exceeded the threshold for seven Beds: 23, 110, 111, 114, 115, 116, 117. Bed 23 was not used in persistence measures because it grossly overpredicted (by one and one-half orders of magnitude) the amount of realized habitat (*e.g.*  $h_{sa} = 60$  hectares and  $h_r = 1$  hectare).

The persistence analysis indicated that patterns varied across beds and models.

The nonsynergistic models showed a greater average number of consecutive months for Bed 116 relative to Bed 115 (Figure 9). The discrepancy between the two nonsynergistic models' average number of continuous months was similar for both Beds 115 and 116 (*e.g.* 53%, 52%, respectively).

The discrepancy between synergistic models was not uniform across beds. The synergistic models exhibited a greater number of months for Beds 114, 115 and 116 relative to Beds 110 and 111. Bed 117 fell between the 'lower' group *e.g.*, Beds 114 and 115 and the 'upper' group *e.g.*, Beds 110 and 111. For Bed 116, the two synergistic models showed almost the same number of months ( $h_s$  model: 43 months;  $h_{sa}$  model: 47 months). The greatest discrepancy occurred between the synergistic models for Beds 111 and 115 (52% for Bed 111 and 46% for Bed 115).

Santa Rosa Beds 115 and 116 were used to compare models because they were characterized by all models. More variation in average number of consecutive months was evident for Bed 115 than Bed 116 (ranges for 115: 7-50 months; ranges for 116: 23-51 months). The  $h_n$  model predicted the lowest average number of consecutive months for Bed 115, increasingly followed by the  $h_{na}$  model, the  $h_s$  model and finally the  $h_{sa}$  model. The pattern was similar for Bed 116, except that the model with the greatest average number of months was the  $h_{na}$  model.

The average number of consecutive months of optimal habitat was then plotted against the OHDs ( $R$ ,  $\text{mean}(SST)$  and  $\text{max}(H)$ ) to examine their role in persistence. A few general observations can be made about the models. First, the range of average number of consecutive months varies across models (Figures 10-12). The  $h_n$  model exhibits the narrowest range (6.1-27 months). The other models have a spanning to 55 months, or the length of the time series. Second, many of the same average number of consecutive months repeat within and across models.

The first plot is of  $\text{mean}(R)$  and average number of consecutive months. The lower end of the  $R$  range is 0.27 for the nonsynergistic models and 0.11 for synergistic models (Figure 10). A wide range of months correspond with low  $R$  values across all models so that a clear relationship does not exist between less rocky locations and persistence. The maximum end of the  $R$  range for all models is 1. For the nonsynergistic models, greater  $R$  values correspond with a lower range of average

number of consecutive months so that locations with the greatest R also tend to be locations of lower persistence. The synergistic models show a stronger correlation between rocky substrate and persistence. Greater values of R tend to correlate with greater average number of consecutive months.

The second plot is of mean SST and the average number of consecutive months of ho (Figure 11). The nonsynergistic models have a narrower range of mean SST (*e.g.* 12-14°C) relative to the synergistic models (*e.g.* 12-15.5°C). The nonsynergistic models do not show a relationship between mean SST and persistence. The greatest number and least number of months span the entire range of mean SST. For the synergistic models, the greatest persistence corresponds with a mean SST range of 12-14°C. Higher values of mean SST ( $SST > 14.3^{\circ}\text{C}$ ) correspond with a lower average number of consecutive months (<30 months) for the synergistic models.

Field studies in southern California have shown that the highest densities of sporophyte recruitment occur at temperatures below 14°C (Deysher and Dean 1986).

The final plot is of maximum H and the average number of consecutive months of ho (Figure 12). The range of maximum H values is similar across all models. The maximum H values corresponding with the greatest average number of consecutive months is narrower for the nonsynergistic models relative to the synergistic models. The nonsynergistic models exhibit a stronger correlation between greater persistence and lower H. Conversely, lower persistence is correlated with greater wave height. The synergistic models do not have as clear of a relationship between persistence and H. A wider relative range of H values corresponds with the greatest average of months for both synergistic models. However, greater H have greater persistence relative to the nonsynergistic models.

To summarize, persistence patterns were not uniform across the Island subregion Beds. Variability existed across beds and between models. Persistence was greater for autocorrelative models relative to their related models. The synergistic models tended to have greater persistence relative to the nonsynergistic models and exhibited persistence patterns that **varied by island**.

Santa Rosa Beds (Beds 114-116) appear almost static in their temporal variability. The average number of consecutive months of optimal habitat approaches the temporal length of the ho time series indicating that only a few months were suboptimal during the time series. The exception is the synergistic Bed 115 where persistence is about 24 months.

The Santa Cruz Beds (Beds 110 and 111) are more dynamic. They have persistence lengths that are shorter. Both models show that Bed 110 has an average length of one year, while Bed 111 is predicted to have one to two year average, depending on the model. Because the hs model converges with the hsa model, Bed 110 has longer periods (at least > 2 months) of suboptimal habitat.

Spatial scales were determined by size of disturbed area while temporal scales were driven by seasonality of disturbance, algal reproductive condition and aperiodic episodes of cool, nutrient-rich waters advected into the patch (Dayton et al. 1984). "Within any given area, the relative patch stability was determined by biological relationships; Between areas, patch stability patterns were attributable to physical differences". (Dayton et al. 1984).

Clearly, persistence of giant kelp's optimal habitat varies spatially across beds and islands. Even though the ability of models to characterize temporal dynamics was not quantitatively evaluated, the models did capture the expected southern California's annual cycle of kelp distribution as well as interannual variability resulting from El Niño and maybe PDO in the study area as well as in portions of the Islands subregion. The nonuniform persistence pattern indicates that areas may have different responses under various climatic and anthropogenic disturbances.

Long term maximum extent composites are frequently used to map static species' distributions, such as kelp. These composites only indicate the potential spatial extent of a species. Does not say the probability that that species will actually be encountered. Many marine species exhibit spatial and temporal scales that are affected by oceanographic conditions. It is well documented that the distribution of kelp can vary greatly on annual scales and is especially affected by El Niño. The 1997-1998 El Niño had a significant effect on several spatial scales. The southern boundary of kelp distribution moved north because reduced upwelling caused water temperatures to increase and nutrient levels to decrease enough to stunt kelp growth and stress the plant to causing kelp beds to deteriorate. Some locations have still not recovered from the El Niño. A maximum extent composite can overpredict the distribution and could identify areas where the species may only exist infrequently. Models such those developed and analyzed in this modeling exercise, could indicate temporal scales of variability and characterize the probability that the species/habitat will persist and actually be encountered. The maximum extent composite characterizes all locations evenly by not providing probability of encountering that habitat.

A characterization of persistence is important in developing MPAs. MPAs are being implemented more frequently across the world to protect and restore marine species and ecosystem linkages, as well as a tool for fisheries management. Essential in designing MPAs are maps of species distributions which are an important consideration when deliberating on locations for MPA establishment that

will provide protection of species of interest and meet the goals of MPAs. Habitat maps are frequently used as a proxy for species distributions. In order to meet MPAs goals, the MPAs must protect the  
Characterization of temporal dynamics and persistence provide a measure of protecting species of interest.

A characterization of temporal variability and persistence is also important in evaluation of MPAs. It can assist in deciphering natural variability due to oceanographic forcing from trends due to biological activity such as urchin grazing and anthropogenic disturbances. Long time series of habitat distributions or oceanographic variables can be extremely valuable in evaluating if declines in canopy cover are a trend potentially caused by anthropogenic disturbances or a part of the interdecadal oceanographic cycle.

This is especially important for kelp. An analysis of the effects of MPAs is important in identifying if MPAs are meeting their goals. A characterization of persistence can play an important role in MPA effectiveness by ensuring the inclusion of the habitat and/or species within the MPA and hence its protection. A greater probability of meeting goals because greater probability of actually offering protection. Also, may offer some prediction of MPA performance. If a species within an MPA exhibits variability over a certain time scale, such as during El Nino events, a characterization of temporal dynamics may assist in distinguishing between MPA performance from natural variability

Potential impact of human activities, such as wastewater and thermal discharge and increased coastal development, are difficult to identify because of a lack of baseline data. Such information would assist resource managers in proving damages and seeking compensation.

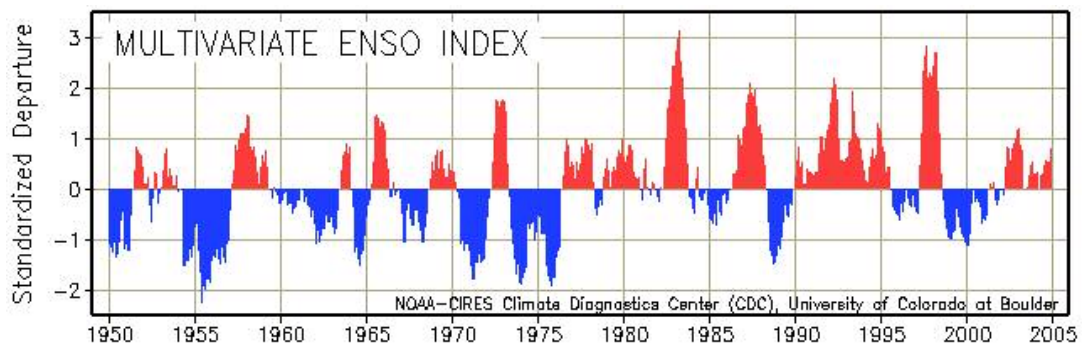


Figure 8. Multivariate ENSO Index (MEI). This index is used to monitor ENSO by basing the index on observed environmental variables over the tropical Pacific. The variables include sea-level pressure, surface winds, sea surface temperature, air temperature, and total cloudiness fraction of the sky (C). MEI is calculated by the NOAA Climate Diagnostics Center.

<http://www.cdc.noaa.gov/people/klaus.wolter/MEI/>

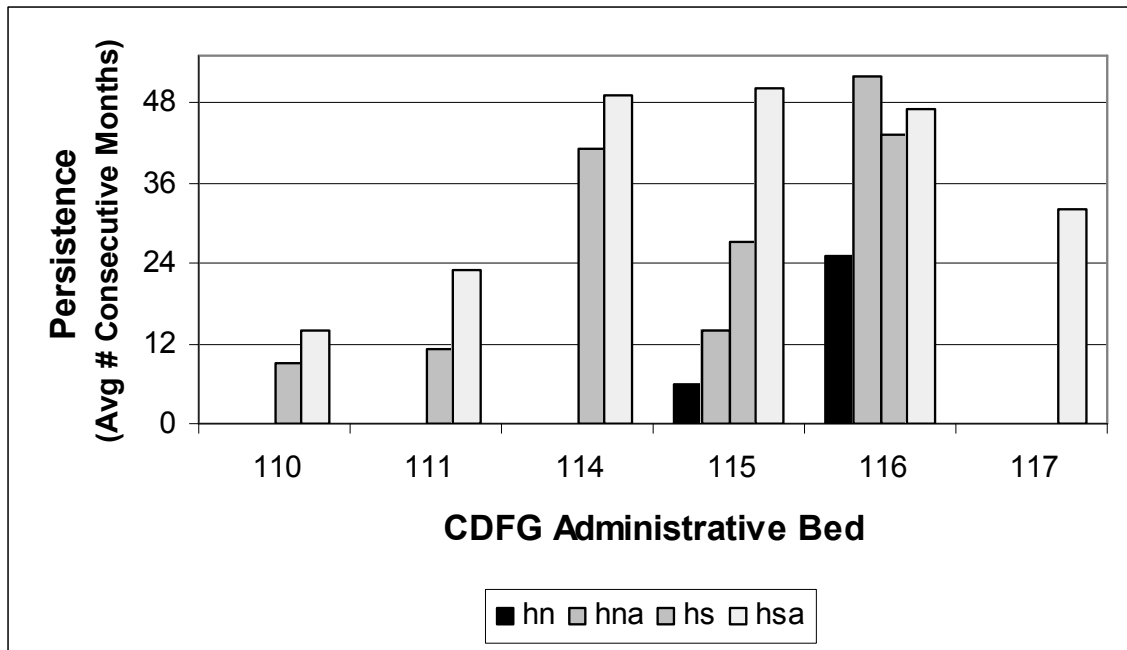


Figure 9. Persistence of CDFG Administrative Beds. Persistence is defined as the average number of consecutive months of optimal habitat ( $h_o$ ) for those CDFG Administrative Beds (Beds) that captured 75% or more of realized habitat,  $h_r$  (defined by the 1999 CDFG kelp aerial survey).

Model abbreviations are:

**hn**--nonsynergistic model      **hna**--nonsynergistic autocorrelative model

**hs**--synergistic model      **hsa**--synergistic autocorrelative model

See *Data and Methods* for a description of models. .

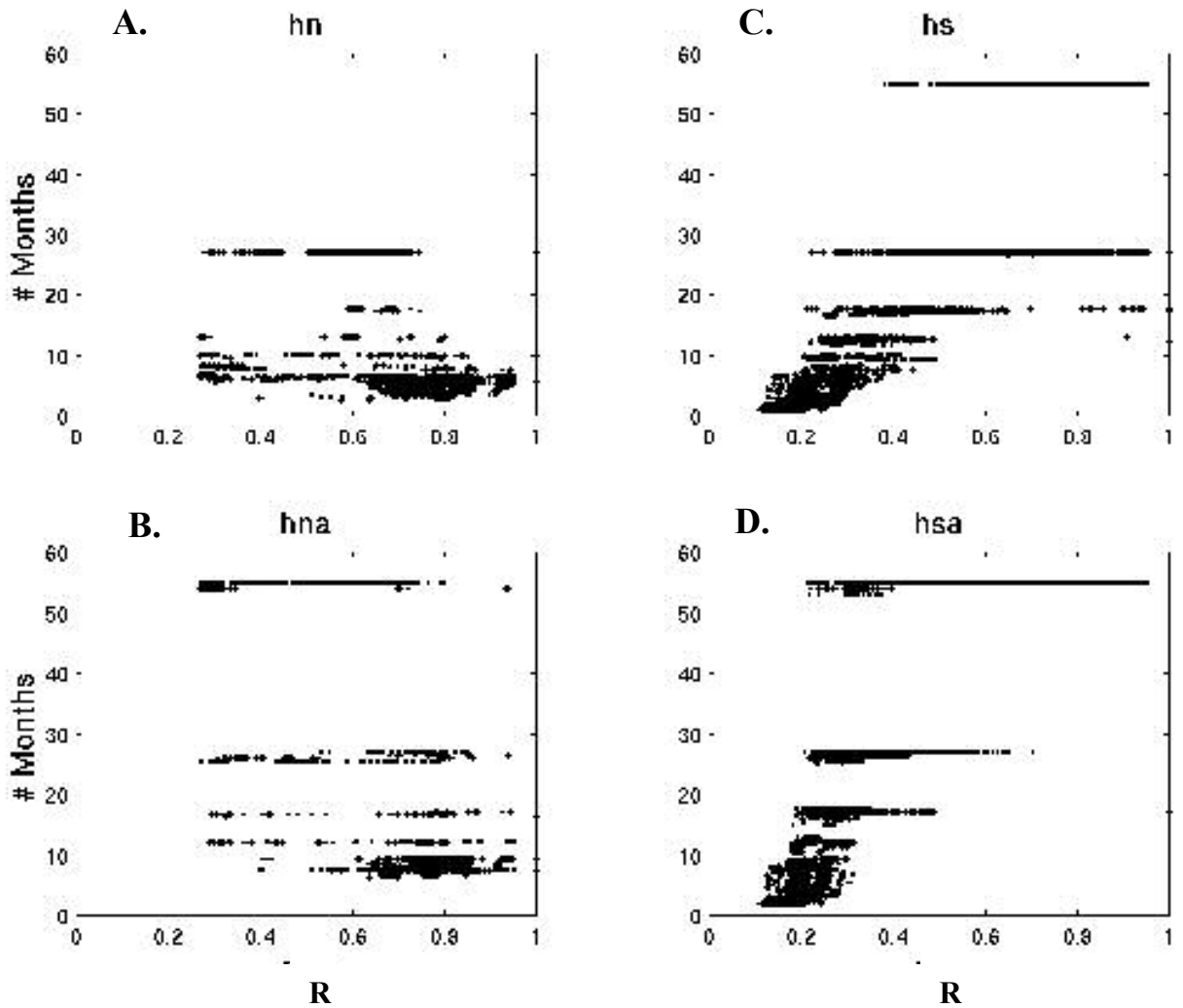


Figure 10. Relationship between persistence and rocky substrate. Persistence is defined as the average number of consecutive months of optimal habitat,  $h_o$ , for locations within CDFG Administrative Beds (Beds) that captured 75% or more of realized habitat,  $h_r$  (defined by the 1999 CDFG kelp aerial survey).  $R$  is the probability of rocky substrate. The four plots are A)  $h_n$  model; B)  $h_{na}$  model; C)  $h_s$  model D)  $h_{sa}$  model. See *Data and Methods* for a description of models and *Discussion* for Beds included in the persistence analysis.

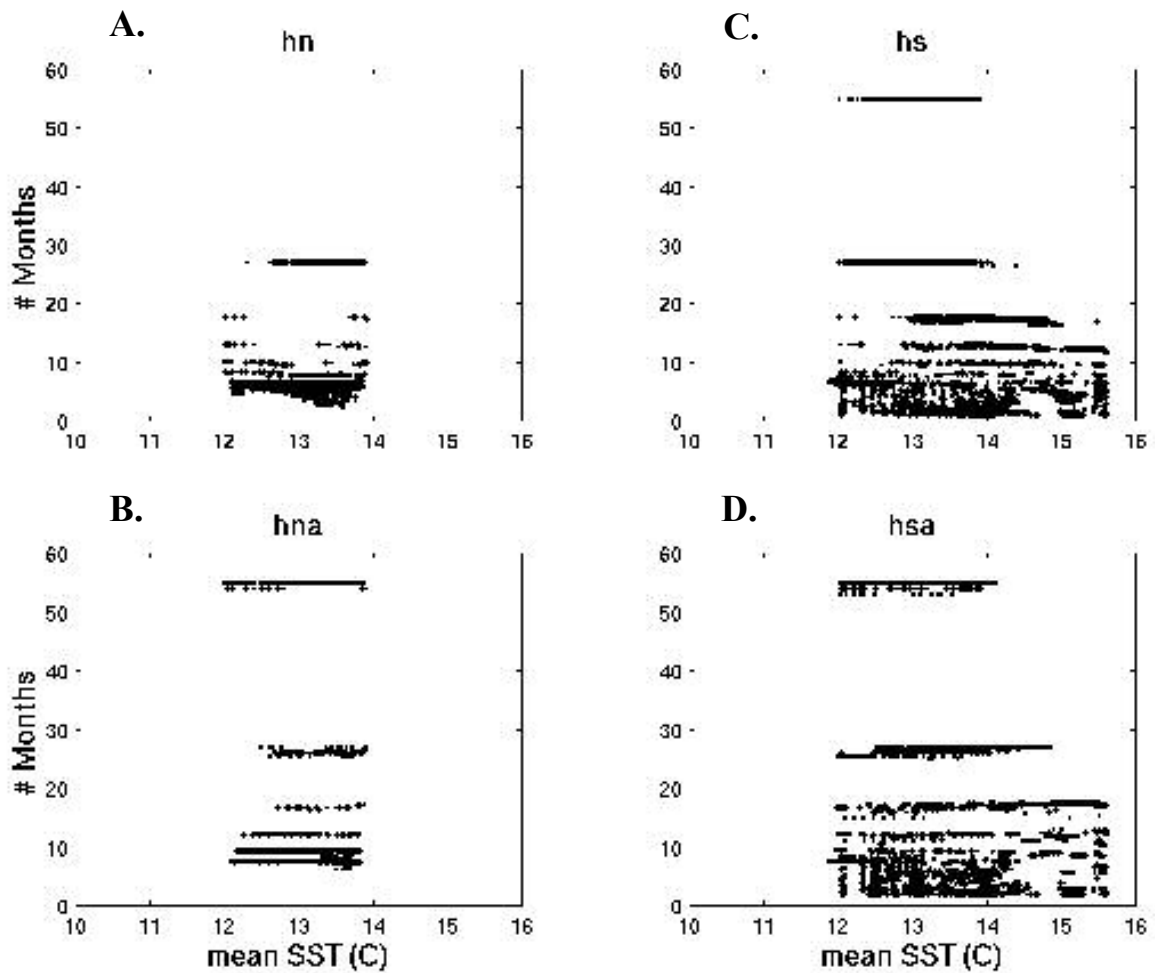


Figure 11. Relationship between persistence and mean sea surface temperature (SST). Persistence is defined as the average number of consecutive months of optimal habitat,  $h_o$ , for locations within CDFG Administrative Beds (Beds) that captured 75% or more of realized habitat,  $h_r$  (defined by the 1999 CDFG kelp aerial survey). Mean SST is calculated using the entire 55-month time series for each location within the selected Beds and Celcius units. The four models' patterns are plotted separately. A)  $h_n$  model; B)  $h_{na}$  model; C)  $h_s$  model D)  $h_{sa}$  model.

See *Data and Methods* for a description of models and *Discussion* for Beds included in the persistence analysis.



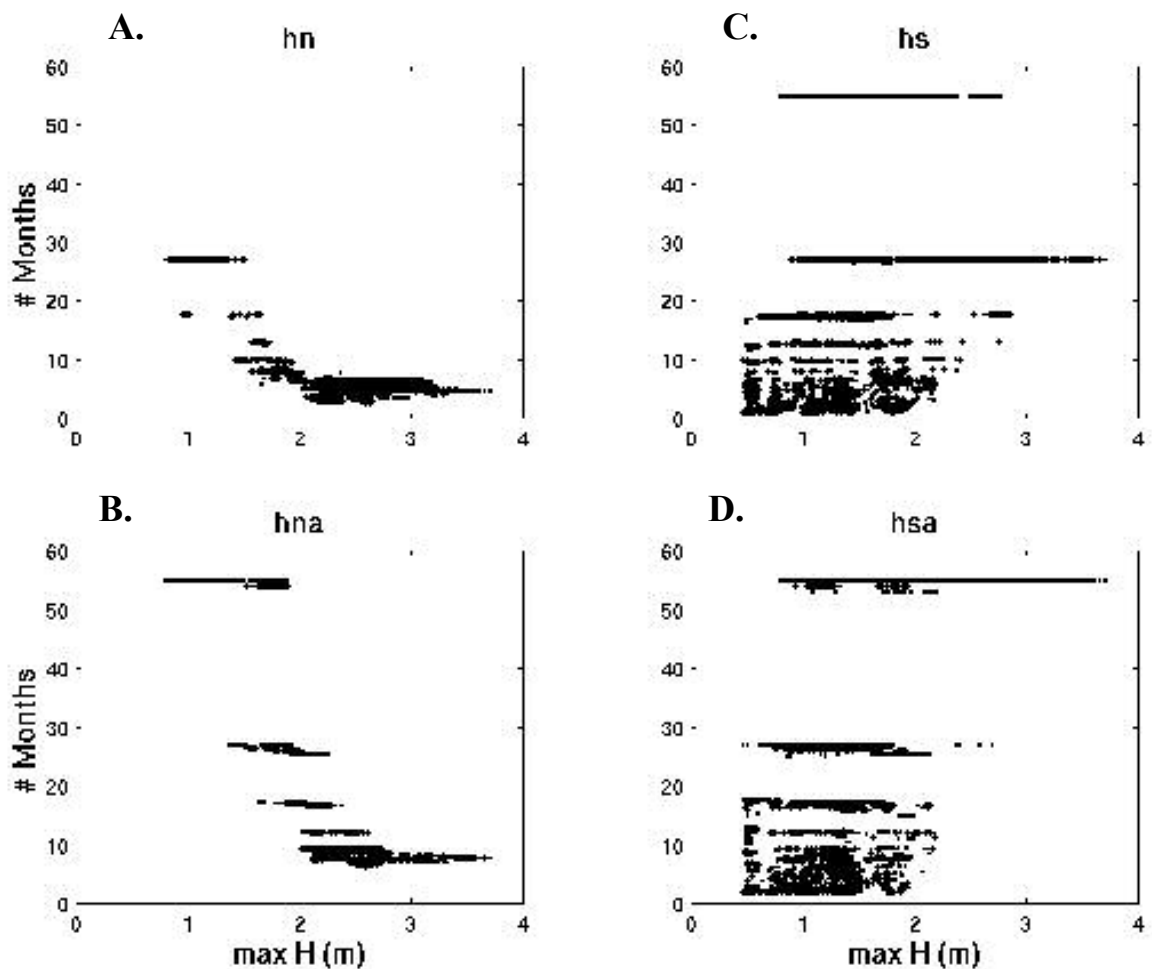


Figure 12. Relationship between persistence and maximum significant wave height (max H). Persistence is defined as the average number of consecutive months of optimal habitat,  $h_o$ , for locations within CDFG Administrative Beds (Beds) that captured 75% or more of realized habitat,  $h_r$  (defined by the 1999 CDFG kelp aerial survey). Max H is the greatest is calculated using the entire 55-month time series for each location within the selected Beds and Celcius units. . The four models' patterns are plotted separately.

A)  $h_n$  model; B)  $h_{na}$  model; C)  $h_s$  model D)  $h_{sa}$  model.

See *Data and Methods* for a description of models and *Discussion* for Beds included in the persistence analysis.

Mean SST is calculated using the entire 55-month time series for each location within the selected Beds and Celcius units. .

The four plots are A)  $h_n$  model; B)  $h_{na}$  model; C)  $h_s$  model D)  $h_{sa}$  model.

See *Data and Methods* for a description of models and *Discussion* for Beds included in the persistence analysis. . .

## 5. Conclusions

- The distribution of optimal habitat was not uniform through time, exhibiting annual to interannual variability
- The synergistic effect between rocky substrate and wave height had a significant impact on annual variability
- Model performed well at islands and in relatively rockier beds
- Persistence patterns were not uniform across the Island Beds
- High resolution seafloor mapping and more frequent canopy aerial surveys are priorities for improving model

## **ACKNOWLEDGEMENTS**

Funding for this project was provided by NOAA NESDIS and the U.C. Marine Council Coastal Environmental Quality Initiative. Data was provided by many researchers and agencies. Ben Waltenberger and Satie Airame at the Channel Islands National Marine Sanctuary provided substrate data and bathymetry. William O'Reilly at the Coastal Data Information Program provided daily averages of wave height and period. Matthew Johnson at the California Department of Fish and Game provided files of 1989 and 1999 surveys of kelp aerial cover. The SB LTER provided the monthly biomass data in a digital, user-friendly format. Their assistance is greatly appreciated.

## 6. Bibliography

- Allee, R. J., M. Dethier, D. Brown, L. Deegan, R. G. Ford, T. F. Hourigan, J. Maragos, C. Schoch, K. Sealey, R. Twilley, M. P. Weinstein and M. Yoklavich. 2000. Marine and Estuarine Ecosystem and Habitat Classification. NOAA Technical Memorandum NMFS-F/SPO-43.
- Bushing W. W. 1994. The influence of topography on the distribution of giant kelp (*Macrocystis pyrifera*) beds around Santa Catalina Island using a geographic information system. In W. L. Halvorson and G. J. Maender (eds.). The Fourth California Islands Symposium: Update on the Status of Resources. Santa Barbara Museum of Natural History, Santa Barbara, CA. pp. 70-82.
- Carr, M. H. 1989. Effects of macroalgal assemblages on the recruitment of temperate reef fishes. *Journal of Experimental Marine Biology and Ecology*. 126: 59-76.
- Carroll, J. C., J. M. Engle, J. A. Coyer and R. F. Ambrose. 1999. Long-term changes and species interactions in a sea urchin-dominated community at Anacapa Island, California. *Proceedings of the Fifth California Islands Symposium*. OCS Study MMS 99-0038.
- Chelton, D. B., P. A. Bernal, and J. A. McGowan. 1982. Large-scale interannual physical and biological interaction in the California Current. *Journal of Marine Research*. 40 (4): 1095-1125.
- Dayton, P. K., and M. J. Tegner. 1984. Catastrophic storms, El Nino, and patch stability in a Southern California kelp community. *Science*. 224: 283-285.
- Dayton, P.K. 1985. Ecology of kelp communities. *Annual Review in Ecology and Systematics*. 16: 215-245.
- Dayton, P. K., M. J. Tegner, P. B. Edwards, and K. L. Riser. 1999. Temporal and spatial scales of kelp demography: The role of oceanographic climate. *Ecological Monographs*. 69(2): 219-250.
- Davinny, J. S. and L. A. Volce. 1978. Effects of sediments on the development of *Macrocystis pyrifera* gametophytes. *Marine Biology*. 48: 343-348.
- Deysher, E. L., and T. A. Dean. 1986. In situ recruitment of sporophytes of the giant kelp, *Macrocystis pyrifera* (L.) C. A. Agardh: effects of physical factors. *Journal of Experimental Marine Biology and Ecology*. 103: 41-63.
- Ecscan. 1989. California Coastal Kelp Resources. Summer 1989. Ecscan Resource Data. P.O. Box 1046. Freedom, California 95019.
- Ford, Jr., R. 2000. Santa Barbara Day Hikes. Published by Shoreline Press, Post Office 3562, Santa Barbara, CA 93130.
- Foster, M.S., Schiel, D. C. 1985. the ecology of giant kelp forests in California: a community profile. *Biological Report*. 85(7.2). U.S. Fish and Wildlife Service, Washington, D.C.
- Graham, M. H., C. Harrold, S. Lisin, K. Light, J. M. Watanabe and M. S. Foster.

1997. Population dynamics of giant kelp *Macrocystis pyrifera* along a wave exposure gradient. *Marine Ecology Progress Series*. 148: 269-279.
- Jackson, G. A. 1977. Nutrients and production of the giant kelp *Macrocystis pyrifera*, off Southern California. *Limnological Oceanography*. 22: 979-995.
- Koenig, C. C., F. C. Coleman, C. B. Grimes, G. Fitzhugh, C. Gledhill, K. M. Scanlon, and M. Grace. 2000. Protection of fish spawning habitat for conservation of warm-temperate reef fish fisheries of shelf-edge reefs of Florida. *Bulletin of Marine Science*. 66(3): 593- 616.
- Ladah, L. B. and J. A. Zertuche-Gonzalez. 1999. Giant kelp (*Macrocystis pyrifera*, Phaeophyceae) recruitment near its southern limit in Baja California after mass disappearance during ENSO 1997-1998. *Journal of Phycology*. 35: 1106-1112.
- Leet, W. S., C. M. Dewees, R. Klingbeil, E. J. Larson. 2001. California's Living Marine Resources: A Status Report. The Resources Agency, California Department of Fish and Game. 592 pp.
- Maravelias, C. D. 1999. Habitat selection and clustering of a pelagic fish: effects of topography and bathymetry on species dynamics. *Canadian Journal of Fisheries and Aquatic Sciences*. 56: 437-450.
- Mumford, T. F. 1992. Characterization of nearshore habitats of Puget Sound, Washington. *Proceedings of the 1st Thematic Conference on Remote Sensing for Marine and Coastal Environments*. New Orleans, LA, USA.
- Mumby, P. J. and A. R. Harborne. 1999. Development of a systematic classification scheme of marine habitats to facilitate regional management and mapping of Caribbean coral reefs. *Biological Conservation*. 88: 155-163.
- National Academy of Science. 2000. *Marine Protected Areas: Tools for Sustaining Ocean Ecosystem*. Committee on the Evaluation, Design, and Monitoring of Marine Reserves and Protected Areas in the United States, Ocean Studies Board, National Research Council.
- National Oceanographic and Atmospheric Administration. 2000. *Marine and estuarine ecosystem and habitat classification*. NOAA Technical Memorandum NMFS-F/SPO-43. National Oceanographic and Atmospheric Administration. Silver Spring, Maryland.
- Otero, M. P. 2002. *Spatial and temporal characteristics of sediment plumes and phytoplankton blooms in the Santa Barbara Channel*. Masters Thesis. University of California, Santa Barbara.
- Rieser, A. 2000. Essential fish habitat as a basis for marine protected areas in the U.S. exclusive economic zone. *Bulletin of Marine Science*. 66(3): 889-899.
- Roemmich, D. and J. McGowan. 1995. Climatic warming and the decline of zooplankton in The California Current. *Science*. 267: 1324-1326.
- Scott, J. S. 1982. Selection of bottom type by groundfishes of the Scotian Shelf.

- Canadian Journal of Fisheries and Aquatic Sciences. 39: 943-947.
- Tegner, M. J., and P. K. Dayton. 1987. El Nino effects on Southern California kelp forest communities. *Advanced Ecological Research*. 17: 243-279.
- Tegner, M. J., P. K. Dayton, P. B. Edwards and K. L. Riser. 1996. Is there evidence of long-term climatic change in Southern California kelp forest communities? *California Cooperative Oceanic Fishery Investigation Report*. 37: 111-126.
- Tegner, M. J., P. L. Haaker, K. L. Riser, and L. I. Vilchis. 2001. Climate variability, kelp forests, and the southern California red abalone fishery. *Journal of Shellfish Research*. 20(2): 755-763.
- Thrush, S. F., J. E. Hewitt, V. J. Cummings, P. K. Dayton, M. Cryer, S. J. Turner, G. A. Funnell, R. G. Budd, C. J. Milburn and M. R. Wilkinson. Disturbance of the marine benthic habitat by commercial fishing: impacts at the scale of the fishery. *Ecological Applications*. 8(3): 866-879.
- Ugoretz, J. 2002. Marine Protected Areas in NOAA's Channel Islands National Marine Sanctuary. Final Environmental Document. California Department of Fish and Game.
- Walters, C. J. and R. Bonfil. 1999. Multispecies spatial assessment models for the British Columbia groundfish trawl fishery. *Canadian Journal of Fisheries and Aquatic Sciences*. 56: 601-628.
- Wolter, K. and M. S. Timlin. 1998. Measuring the strength of ENSO events: How does the 1997/98 rank? *Weather*. 53: 315-324.
- Zimmerman, R. C. and J. N. Kremer. 1984. Episodic nutrient supply to a kelp forest ecosystem in southern California. *Journal of Marine Research*. 42: 591-604.
- Zimmerman, R. C. and J. N. Kremer. 1986. In situ growth and chemical composition of the giant kelp, *Macrocystis pyrifera*: response to temporal changes in ambient nutrient availability. *Marine Ecology Progress Series*. 27: 277-285.